Potassium niobate nanoscrolls incorporating rhodium hydroxide nanoparticles for photocatalytic hydrogen evolution

Renzhi Ma,[ab] Yoji Kobayashi,[b] W. Justin Youngblood[b] and Thomas E. Mallouk*[b]

Received 14th July 2008, Accepted 18th September 2008
First published as an Advance Article on the web 5th November 2008
DOI: 10.1039/b812003j

Well-dispersed rhodium trihydroxide nanoparticles (below 1 nm) were deposited into the interlayer galleries of scrolled $K_4Nb_6O_{17}$ nanosheets. The unmodified nanoscrolls are good catalysts for UV light-driven hydrogen evolution from aqueous methanol solutions, and their activity can be significantly improved by anchoring a small amount (0.1 wt% Rh) of $Rh(OH)_3$ or Rh_2O_3 to the surface. The high hydrogen generation rate achieved in this system, 1480 μmol/h per 1g of catalyst, shows promise towards overall water splitting using these catalytic composites.

Introduction

Layered $K_4Nb_6O_{17}$ is composed of corrugated sheets of edge-sharing NbO_6 octahedra. In each layer, the top and bottom faces are different from each other, giving rise to two different interlayer environments for hydration and intercalation.[1] The asymmetry is regarded as the driving force leading to spontaneous scrolling when proton-exchanged $H^+/K_4Nb_6O_{17}$ (or $H_xK_{4-x}Nb_6O_{17}$, $x \approx 3$) is exposed to aqueous tetra (n-butyl)ammonium hydroxide (TBA^+OH^-) and exfoliated.[2] $K_4Nb_6O_{17}$ loaded with interlayer Ni or Pt clusters has shown high photocatalytic activity for the photolysis of water and alcohols under UV light.[3] Porous composites obtained by exfoliation of $H^+/K_4Nb_6O_{17}$ and subsequent precipitation of MgO fine particles also showed high photocatalytic activity for H_2 evolution from various aqueous alcohol solutions.[4] The properties of surface-modified, platinized $K_4Nb_6O_{17}$ in the photolysis of HI with visible light have also been investigated.[5] However, expansion of $K_4Nb_6O_{17}$ interlayer gallery by silica pillaring was not successful though it could be accomplished for clays and $KCa_2Nb_3O_{10}$.[6]

In our previous report, the uniform dispersion of $Rh(OH)_3$ nanoparticles, which can be converted to Rh_2O_3 by calcination, in the interlayer galleries of exfoliated–restacked $KCa_2Nb_3O_{10}$ and $HCa_2Nb_3O_{10}$ was achieved, which brought about a high rate of H_2 evolution under UV light.[7] We hypothesized that $Rh(OH)_3$ and Rh_2O_3 nanoparticles were anchored to the calcium niobate sheets by covalent interactions, i.e., by Rh–O–Nb bonding. This motivated us to investigate another Rh–O–Nb system, specifically based on $K_4Nb_6O_{17}$ nanoscrolls, to look for the possibility of expanding the interlayer space with active $Rh(OH)_3$ nanoparticles and interesting photocatalysis functionalities.

[a]*Nanoscale Materials Center, National Institute for Materials Science (NIMS), Namiki 1-1, Tsukuba, Ibaraki, 305-0044, Japan. E-mail: MA.Renzhi@nims.go.jp; Fax: +81 29 854 9061; Tel: +81 29 860 4124*
[b]*Department of Chemistry and Materials Research Institute, The Pennsylvania State University, University Park, Pennsylvania, 16802, USA. E-mail: tom@chem.psu.edu; Fax: +1 814 863 8403; Tel: +1 814 863 9637*

Experimental

Materials preparation and characterization

Synthetic $K_4Nb_6O_{17}$ crystals with a typical size of 1–10 μm were obtained by solid calcination of K_2CO_3 and Nb_2O_5.[2] 1.0 g $K_4Nb_6O_{17}$ was stirred in 300 ml of 1M HCl solution for 4 days to produce $H_xK_{4-x}Nb_6O_{17}$ ($x \approx 3$); presumably the remaining K^+ ions reside mainly in the slowly exchanging interlayer galleries. The acid solution was renewed 3 times to promote a complete exchange. The proton-exchanged solid $H_xK_{4-x}Nb_6O_{17}$ (0.2 g) was shaken in 50 mL of aqueous TBAOH solution (25 mM, pH ~11) for 24 h to obtain a colloidal suspension of exfoliated $(TBA)_xK_{4-x}Nb_6O_{17}$. In order to incorporate rhodium hydroxide, the colloidal suspension was combined with different volumes of aqueous $RhCl_3$ (8.2 mM) solution and vigorously stirred for another day. The added amount of $RhCl_3$ corresponded to 0.1, 1.0 and 10.0 wt% Rh loading of $H_xK_{4-x}Nb_6O_{17}$, respectively. The yellowish suspension was then poured into 50 mL of 2 M KOH solution. As TBA^+ ions were replaced by K^+, the exfoliated $(TBA)_xK_{4-x}Nb_6O_{17}$ was instantly flocculated into a wool-like sediment. The precipitated product was centrifuged and rinsed with copious amounts of water to remove excess KOH. A portion of the $Rh(OH)_3/K_4Nb_6O_{17}$ was calcined at 623 K in air for 1 h to convert deposited $Rh(OH)_3$ into Rh_2O_3. After calcination, a color change from yellow to grey (0.1, 1.0 wt%) or dark brown (10.0 wt%), indicating the formation of Rh_2O_3, was observed. $Rh_2O_3/K_4Nb_6O_{17}$ was further acid-exchanged with 1M HNO_3 to obtain $Rh_2O_3/H_xK_{4-x}Nb_6O_{17}$.

X-Ray powder diffraction (XRD) patterns were obtained with a Philips X'Pert MPD diffractometer (monochromatized Cu Kα 0.15418 nm). Transmission electron microscope (TEM) images were obtained using a Philips 420 T microscope at an accelerating voltage of 120 kV and a JEOL JM-2010 microscope (operating at 200 kV). Samples for TEM observation were prepared by depositing a drop of ethanol-dispersed sample suspensions onto a carbon-coated copper grid and air-dried.

Photocatalysis

5.0 mg catalyst was suspended in 2.0 mL of aqueous 10 vol% methanol solution in a quartz reaction cell (5.0 mL) sealed with

a rubber septum. The sample was purged with Ar for 10 min. The reaction cell was then placed in an outer jacket, where an Ar gas flow was introduced to prevent air contamination during the photocatalytic reaction. The suspension, under constant stirring, was irradiated using a UV light source (a 300 W Xe lamp). Throughout the reaction, a headspace gas sample (100 microliter) was taken using a syringe at different time intervals. The gas sample was analyzed for hydrogen content by gas chromatography (GC) using a thermal conductivity detector and a 5A molecular sieve column.

Results and discussion

1. Exfoliated–scrolled $K_4Nb_6O_{17}$ intercalating $Rh(OH)_3$ nanoparticles

Fig. 1 shows TEM images of the freshly exfoliated $(TBA)_xK_{4-x}Nb_6O_{17}$. The sample was imaged by directly dropping the colloidal suspension onto a carbon-coated copper grid. TEM images revealed a mixure of exfoliated nanosheets and scrolled tubular objects, i.e., nanoscrolls. Fig. 1b displays a selected area view of some nanoscrolls. They are approximately 30 nm in diameter and a few hundred nm in length, consistent with previous observations.[2] The top-right inset in Fig. 1b shows an individual nanoscroll with an apparent hollow core and an observed wall thickness of ~5 nm. High resolution observations reveal that the wall thicknesses of the nanoscrolls generally fall between 3and 8 nm, corresponding to 3–10 radial layers.

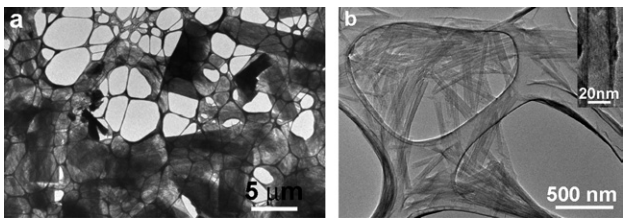

Fig. 1 $(TBA)_xK_{4-x}Nb_6O_{17}$ nanosheets/nanoscrolls upon exfoliation in aqueous TBAOH solution. (a) Low-magnification overview; and (b) selected area view of nanoscrolls; (top-right inset) an individual nanoscroll.

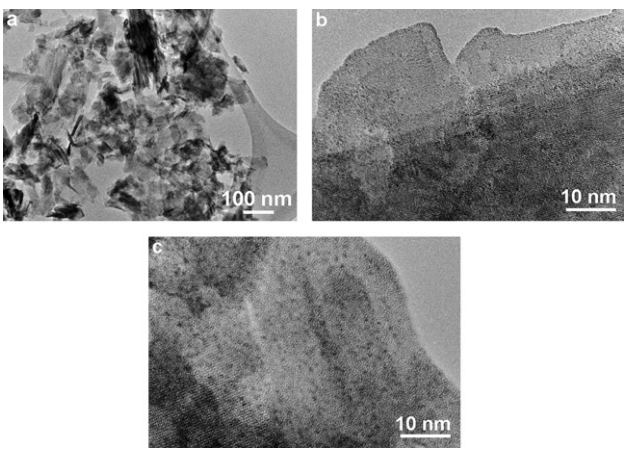

Fig. 2 TEM images of restacked $Rh(OH)_3/K_4Nb_6O_{17}$. (a) Overview; (b) 1wt% loading; and (c) 10 wt% loading.

Fig. 2 shows TEM images of restacked $Rh(OH)_3/K_4Nb_6O_{17}$. As can be seen in Fig. 2a, the solid is still a typical mixture of sheets and nanoscrolls, though it appears that the fraction of nanoscrolls is not so predominant as observed in exfoliated $(TBA)_xK_{4-x}Nb_6O_{17}$. It is suspected that some particles are unscrolled into nanosheets during the subsequent treatment involving vigorous stirring and restacking with concentrated KOH. It has been noted that there is relatively little free energy difference between the nanoscrolls and nanosheets.[2] Fig. 2b displays restacked nanosheets of $Rh(OH)_3/K_4Nb_6O_{17}$ with 1wt% Rh loading. Darker-contrast nanoparticles can be discerned. With a higher loading of 10 wt% (Fig. 2c), a homogeneous distribution of abundant nanoparticles is apparent. The average sizes of the nanoparticle were estimated to be 0.5 ± 0.2 nm and 0.8 ± 0.3 nm for 1 wt% and 10 wt% Rh loading, respectively. Energy dispersive X-ray spectral (EDS) surveys of the samples give an average atomic ratio for K:Nb at 44:56, close to the stoichiometry (K:Nb = 40:60) in $K_4Nb_6O_{17}$. EDS analysis also identified uniform dispersion of Rh in all sampled areas. For a nominal 10 wt% Rh loading sample, EDS quantification results yield a typical atomic ratio for Rh:Nb at 12:88, *ca.* 9.6 wt% Rh loading of $H_xK_{4-x}Nb_6O_{17}$. All the microanalytical data confirm the incorporation of a designated amount of Rh into the exfoliated–scrolled $K_4Nb_6O_{17}$.

Fig. 3 compares XRD powder patterns for proton-exchanged $H_xK_{4-x}Nb_6O_{17}$ prior to exfoliation and the exfoliated–restacked products with different loadings of Rh (0, 0.1, 1, 10 wt%). The layered structure of $K_4Nb_6O_{17}$ is believed to be preserved during the exfoliation and scrolling, as manifested by the 040 basal reflections. Moreover, *hkl* reflections generally become extinct whereas the in-plane reflections such as 002 and 400 are retained, indicating an intact host structure of $K_4Nb_6O_{17}$ during the process. It is noteworthy that no diffraction peaks attributed to $Rh(OH)_3$ were observed. This is consistent with the very small particle size (Fig. 2) and with the non-crystalline nature of the $Rh(OH)_3$ nanoparticles. The interlayer spacing (040) of exfoliated–restacked $K_4Nb_6O_{17}$ without Rh loading is approximately 8.6 Å, which is increased to 9.1, 9.5 and 10.6 Å for 0.1 wt%, 1 wt% and 10 wt% loadings, respectively. These correspond to an expansion of 0.5, 0.9, and 2 Å, respectively, indicating the size of intercalated $Rh(OH)_3$ nanoparticles increases accordingly with a higher loading. Unlike $KCa_2Nb_3O_{10}$, $K_4Nb_6O_{17}$ nanosheets are corrugated in the sheet

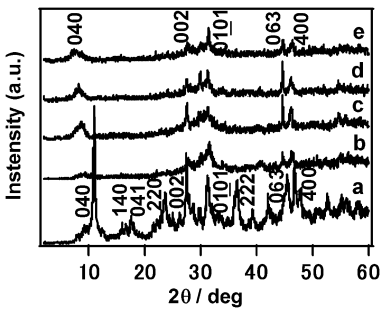

Fig. 3 XRD patterns of (a) proton-exchanged $H_xK_{4-x}Nb_6O_{17}$; (b) exfoliated–scrolled $K_4Nb_6O_{17}$ (no Rh loading); (c) $Rh(OH)_3/K_4Nb_6O_{17}$ (0.1wt%); (d) $Rh(OH)_3/K_4Nb_6O_{17}$ (1wt%); and (e) $Rh(OH)_3/K_4Nb_6O_{17}$ (10 wt%).

normal direction. It is difficult to calculate the gallery height, by simply subtracting the atomic thickness of the niobate layer, to gauge $Rh(OH)_3$ size. Instead, the interlayer expansion relative to exfoliated–restacked $K_4Nb_6O_{17}$ without Rh loading was used to estimate the gallery height. As the ionic radius of K^+ is 1.38 Å,[8] the expansion in the interlayer spacing can be converted into an intercalation of $Rh(OH)_3$ nanoparticles with sizes of 3.26 (2 × 1.38 + 0.5), 3.66 (2 × 1.33 + 0.9), and 4.76 (2 × 1.33 + 2.0) Å, respectively. The values are close to but somewhat smaller than those estimated from statistical TEM observations. The deviation might imply that the particles are not in a strict spherical shape, possibly in a disc-like shape, namely, slightly thinner in height but somewhat elongated in the in-plane directions.

2. Photocatalytic activity

Time courses of H_2 evolution on different $K_4Nb_6O_{17}$ samples with and without Rh loading are shown in Fig. 4. For synthetic $K_4Nb_6O_{17}$ crystals, the rate of H_2 generation is rather low, 0.7 μmol/h or a converted 140 μmol/h per 1g of catalyst. After proton-exchange and exfoliation, the rate for the restacked $K_4Nb_6O_{17}$ significantly increases to 5.6 μmol/h, or 1120 μmol/h per 1g of catalyst. This agrees well with the previous reports asserting that reactants (methanol and water) have better access to the more hydrated galleries.[3,4] It is also apparent that the nanoscrolls have much higher surface area and open channels than synthetic layered $K_4Nb_6O_{17}$. With the intercalation of 0.1 wt% $Rh(OH)_3$, the rate is increased to 6.7 μmol/h, or 1340 μmol/h per 1g of catalyst, about a ~20% increase. This is strikingly higher than the H_2 generation rate (275 μmol/h per 1 g of catalyst) under similar conditions for $Rh(OH)_3/KCa_2Nb_3O_{10}$ (0.1 wt%).[7]

When the Rh loading was increased to 1 wt%, the rate decreased to 3.2 μmol/h. It further drops to 2.6 μmol/h for a higher loading (10 wt%) of $Rh(OH)_3$. It appears that 0.1 wt% loading is an optimum combination. This is consistent with results obtained with Rh-loaded $KCa_2Nb_3O_{10}$[7] and Ni-loaded $K_4Nb_6O_{17}$,[3a] in which the activities also decrease gradually when the loading is above 0.1 wt%. The reduced activity at higher $Rh(OH)_3$ loading, even below that of Rh-free nanoscrolls, is derived from an optical inner filter effect of strongly UV-absorbing $Rh(OH)_3$. A simple calculation based on the extinction coefficient of aqueous $Rh(OH)_3$ (0.1 mM^{-1} cm^{-1} at 350 nm)[9] results in 43% loss of UV absorption by 10 wt% $Rh(OH)_3$ loading (2.42 mM $Rh(OH)_3$) in a 1 cm cell.

$$\begin{aligned}\text{Percent transmittance}/100 &= 10^{-\text{absorbance}} \\ &= 10^{-(0.1\times 2.42\times 1)} \\ &= 0.57\end{aligned}$$

This is in semi-quantitative agreement with the reduction of the H_2 generation rate from 5.6 μmol/h (no Rh loading) to 2.6 μmol/h (10 wt% Rh).

After calcination at 623 K, $Rh(OH)_3$ was transformed into Rh_2O_3, which was evidenced by a color change to brown. Again, no XRD peaks for Rh_2O_3 were detected as the nanoparticles do not form crystalline aggregates. Although Rh_2O_3 is expected to be a better catalyst than $Rh(OH)_3$, the catalytic activity for the sample with 0.1 wt% Rh_2O_3 loading after calcination remained essentially unchanged. This is possibly due to the effect of dehydration in the calcined sample. After another acid-exchange procedure, the hydrogen generation rate for 0.1 wt% Rh_2O_3, increased to ~7.4 μmol/h, or 1480 μmol/h per 1g of catalyst. This suggests that proton-exchange and hydration enable better access of methanol and water to the interlayer galleries of the restacked sheets and nanoscrolls.

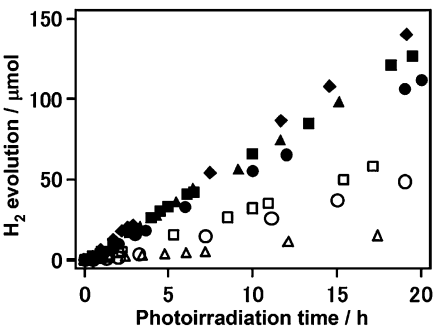

Fig. 4 Time course of hydrogen evolution on synthetic $K_4Nb_6O_{17}$ crystals (△), exfoliated–scrolled $K_4Nb_6O_{17}$ without Rh loading (●), $Rh(OH)_3/K_4Nb_6O_{17}$ (0.1wt%, ■), $Rh(OH)_3/K_4Nb_6O_{17}$ (1wt%, □), $Rh(OH)_3/K_4Nb_6O_{17}$ (10 wt%, ○), $Rh_2O_3/K_4Nb_6O_{17}$ (0.1wt%,▲) and $Rh_2O_3/H_xK_{4-x}Nb_6O_{17}$ (0.1wt%, ◆). Reaction conditions: 5 mg catalyst and 10 vol% aqueous methanol solution under UV irradiation from a 300 W Xe lamp.

Conclusions

In summary, a uniform deposition of $Rh(OH)_3$ nanoparticles (below 1 nm) into the interlayer galleries of $K_4Nb_6O_{17}$ nanoscrolls has been achieved through an exfoliating–restacking procedure, demonstrating an efficient way to expand the interlayer space with active catalyst nanoparticles and to control the dispersion on semiconductor host sheets. The photocatalysis results indicate that the activity of exfoliated–restacked $K_4Nb_6O_{17}$ can be improved by anchoring a suitable amount (0.1 wt% Rh) of $Rh(OH)_3$ or Rh_2O_3. The high hydrogen generation rate achieved in this system is noteworthy, because it has been shown that hydrogen evolution is the rate-determining process in visible-light overall water splitting using semiconducting oxynitride photocatalysts.[10] In that work, Rh-based nanoparticles were the hydrogen evolving catalysts of choice because, with suitable modification, they do not catalyze the O_2–H_2 recombination reaction. Further work is being directed towards overall water splitting using similar catalytic composites based on dye-sensitized nanoscrolls.[11]

Acknowledgements

This work was supported by the Office of Basic Energy Sciences, Department of Energy under contract DE-FG02-07ER15911. R.M. thanks NIMS for support in an overseas dispatch program. W.J.Y. thanks the donors of the ACS Petroleum Research Fund for support in the form of a postdoctoral fellowship.

References

1 (*a*) K. Nassau, J. W. Shiever and J. L. Bernstein, *J. Electrochem. Soc.*, 1969, **116**, 348; (*b*) G. Lagaly and K. Beneke, *J. Inorg. Nucl. Chem.*, 1976, **38**, 1513; (*c*) N. Kinomura, N. Kumada and F. Muto, *J. Chem. Soc., Dalton Trans.*, 1985, **11**, 2349; (*d*) M. Gasperin and M. T. Le Bihan, *J. Solid State Chem.*, 1982, **43**, 346.

2 (*a*) R. Abe, K. Shinohara, A. Tanaka, M. Hara, J. N. Kondo and K. Domen, *J. Mater. Res.*, 1998, **13**, 861; (*b*) G. B. Saupe, C. C. Waraksa, H.-N. Kim, Y. J. Han, D. M. Kaschak, D. M. Skinner and T. E. Mallouk, *Chem. Mater.*, 2000, **12**, 1556; (*c*) Y. Kobayashi, H. Hata, M. Salama and T. E. Mallouk, *Nano Lett.*, 2007, **7**, 2142.

3 (*a*) K. Domen, A. Kudo, M. Shibata, A. Tanaka, K. Maruya and T. Onishi, *Chem. Commun.*, 1986, 1706; (*b*) A. Kudo, K. Sayama, A. Tanaka, K. Asakura, K. Domen, K. Maruya and T. Onishi, *J. Catal.*, 1989, **120**, 337; (*c*) K. Sayama, A. Tanaka, K. Domen, K. Maruya and T. Onishi, *J. Catal.*, 1990, **124**, 54; (*d*) K. Sayama, A. Tanaka, K. Domen, K. Maruya and T. Onishi, *J. Phys. Chem.*, 1990, **95**, 1345; (*e*) A. Tanaka, J. N. Kondo and K. Domen, *Crit. Rev. Surf. Chem.*, 1995, **5**, 305.

4 (*a*) R. Abe, K. Shinohara, A. Tanaka, M. Hara, J. N. Kondo and K. Domen, *Chem. Mater.*, 1997, **9**, 2179.

5 (*a*) Y. I. Kim, S. Salim, M. J. Hug and T. E. Mallouk, *J. Am. Chem. Soc.*, 1991, **113**, 9561; (*b*) Y. I. Kim, S. J. Atherton, E. S. Brigham and T. E. Mallouk, *J. Phys. Chem.*, 1993, **97**, 11802; (*c*) G. B. Saupe, T. E. Mallouk, W. Kim and R. H. Schmehl, *J. Phys. Chem.*, 1997, **101**, 2508.

6 Y. Ebina, A. Tanaka, J. N. Kondo and K. Domen, *Chem. Mater.*, 1996, **8**, 2534.

7 H. Hata, Y. Kobayashi, V. Bojan, W. J. Youngblood and T. E. Mallouk, *Nano Lett.*, 2008, **8**, 794.

8 R. D. Shannon, *Acta Crystallogr.*, 1976, **A32**, 751.

9 (*a*) J. C. Armstrong, G. R. Choppin, *Radiochemistry of Rhodium*, United States Atomic Energy Commission, 1965; (*b*) C. K. Jorgensen, *Acta Chem. Scand*, 1956, **10**, 500.

10 K. Maeda, H. Hashiguchi, H. Masuda, R. Abe and K. Domen, *J. Phys. Chem. C*, 2008, **112**, 3447.

11 K. Maeda, M. Eguchi, W. J. Youngblood and T. E. Mallouk, submitted for publication.